Proposal of Contour Line Model for High-Speed End Milling Simulation

Nishida, Isamu

Shirase, Keiichi

(Citation)
International Journal of Automation Technology,14(1):38-45

(Issue Date)
2020-01-05

(Resource Type)
journal article

(Version)
Version of Record

https://doi.org/10.20965/ijat.2020.p0038

Paper:

Proposal of Contour Line Model for High-Speed End Milling Simulation

Isamu Nishida[†] **and Keiichi Shirase**

Kobe University
1-1 Rokko-dai, Nada-ku, Kobe, Hyogo 657-8501, Japan
[†]Corresponding author, E-mail: nishida@mech.kobe-u.ac.jp
[Received June 5, 2019; accepted September 30, 2019]

A contour line model for end milling simulation, which realizes high-speed arithmetic processing by reducing memory usage, is proposed. In this model, a 3-dimensional shape can be expressed by superimposing the contour lines of the cross-sections obtained by dividing the workpiece along any axial direction. Therefore, the memory usage is reduced compared to a Z-map model or a voxel model as the interior information of the object can be eliminated. The contour line model can also be applied to complicated shapes having overhangs. Furthermore, cutting volume can be calculated from the interference area enclosed by two contour lines of the workpiece and the tool cross-sections. The workpiece shape can be changed by eliminating the interference area. In the contour line model, cutting force can also be predicted with an instantaneous rigid force model using the uncut chip thickness for each cutting edge from the positional relationship between the interference area and the cutting edge. To validate the proposed model, cutting experiments were conducted, which confirmed that the predicted machining shape had good agreement with the actual machined shape. Furthermore, it was confirmed that the cutting force can be predicted accurately.

Keywords: end milling simulation, contour line, cutting force simulation, NC machining

1. Introduction

To improve machining efficiency, it is necessary to predict machining status and optimize cutting conditions. Previous studies have been conducted to discuss cutting status. These studies describe models that include the instantaneous rigid force model [1–4], the chip flow model based on the piling up of the orthogonal cuttings [5], and cutting force simulation using the finite element method (FEM). Among these models, the instantaneous rigid force model makes it easier to properly calculate cutting forces from the interference area between the tool cutting edge and workpiece. However, cutting force prediction is difficult when the change in machining shape is complicated and the contact state of the tool cutting edge and workpiece is not uniform, because this method needs an accurate uncut chip thickness to make the prediction.

Methods for uncut chip thickness calculation, when the machining shape is complex, have been proposed according to various models. The parallel slicing method (PSM) uses a discretized 2-dimensional form of the 3-dimensional geometry found in a solid boundary representation (B-Rep) model [6, 7]. In the PSM, the removal volume is generated and the workpiece is updated in the solid B-Rep model. Therefore, a computer-aided design (CAD) engine is necessary to analyze the intersection curve between the tool and workpiece. The other models analyze the interference area by representing the whole workpiece discretely from the beginning without a CAD engine. The Z-map model discretely represents a workpiece with a plurality of lines in the Z-axis direction arranged at equal intervals on the XY-plane [8–10]. In this model, although it is possible to analyze using a relatively small amount of memory usage, a workpiece with overhangs cannot be easily expressed. The voxel model discretely represents the inside of a workpiece with a cube called a voxel [11–22]. In this model, although it is possible to express a workpiece with overhangs, a large amount of memory usage is required for a large size workpiece and highly-accurate analysis, and the calculation time is quite large to detect the interference area between the tool and workpiece.

In this study, a contour line model, where the workpiece is minutely divided on the plane along any axial direction and the contour line of the cross-section of the workpiece is superimposed, is proposed to realize end milling simulation with high-speed arithmetic processing by reducing the memory usage. A cutting experiment is conducted to validate the effectiveness of the proposed model.

2. End Milling Simulation Using Contour Line Model

2.1. Contour Line Model

For end milling simulation, it is necessary to detect the interference area between the tool and workpiece, and change the workpiece shape by eliminating the inter-

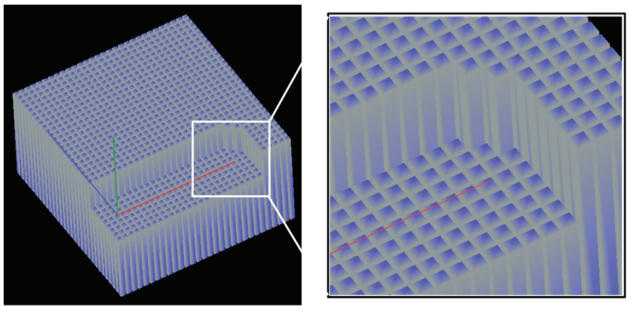

Fig. 1. Workpiece representation referring the Z-map model.

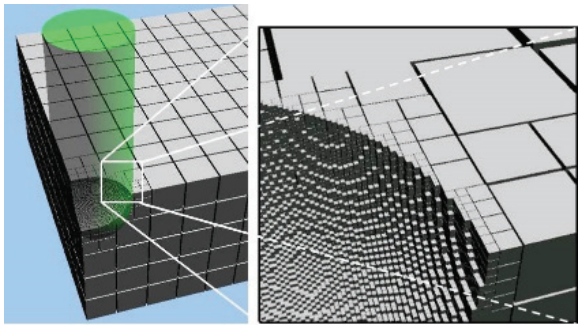

Fig. 2. Workpiece representation referring the voxel model.

ference area. Previous studies have analyzed the interference area by representing the whole workpiece discretely from the beginning without a CAD engine. Methods using the Z-map model or voxel model have been proposed for representing the workpiece shape. The Z-map model discretely represents a workpiece with a plurality of lines in the Z-axis direction arranged at equal intervals on the XY-plane, as shown in **Fig. 1**. In this model, analysis can be performed with a relatively low memory usage. Furthermore, the interference area between the tool and workpiece can also be easily calculated. However, the Z-map model generally only possesses the height information in the Z-axis direction, thus, representing complicated shapes having overhangs is difficult. On the other hand, the voxel model discretely represents the inside of a workpiece with a cube called a voxel, as shown in **Fig. 2**. In this model, complicated shapes having overhangs can be easily represented. Furthermore, the interference area between the tool and workpiece can also be easily calculated by extracting the voxels present in the tool. However, the memory usage increases for a large size workpiece and highly-accurate analysis requirement because the 3-dimensional shape is filled and represented with minute voxels. Thus, the calculation time to detect the interference area between the tool and workpiece also increases.

In this study, to reduce the memory usage and realize high-speed arithmetic processing, a method representing the workpiece shape using the contour line model is proposed. In the contour line model, the workpiece is minutely divided on the plane along any axial direction and the contour line of the cross-section is superimposed

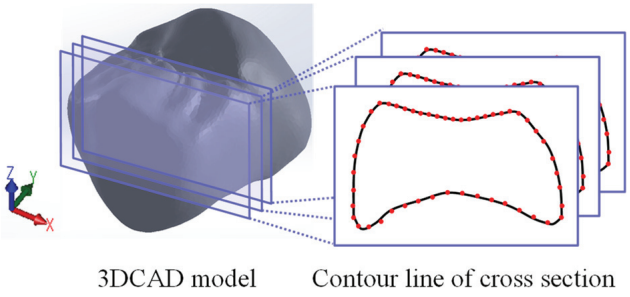

Fig. 3. Workpiece representation using the contour line model.

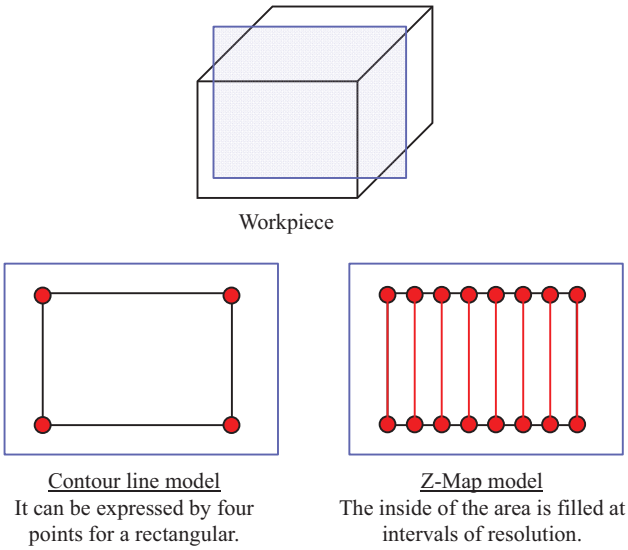

Fig. 4. Comparison of CPU memory usage between the contour line model and Z-map model.

and represented discretely, as shown in **Fig. 3**. The contour line on the divided plane is also represented by a polygon with a minimum number of points, as shown in **Fig. 4**. Therefore, the memory usage of the contour line model can be reduced in comparison to the Z-map and voxel models as the interior information of the 3-dimensional object can be eliminated. Furthermore, it is possible to apply the contour line model to complicated shapes having overhangs, as shown in **Fig. 5**.

2.2. Detection of Interference Area Between Workpiece and Tool, and Change of Workpiece Shape

For end milling simulation, it is necessary to detect the interference area between the workpiece and tool, and to change the workpiece shape by eliminating the interference area. In the case of the Z-map model, the interference area can be calculated by extracting the plurality of lines existing in the tool, as shown in **Fig. 6(a)**. The change of the workpiece shape can be expressed by updating the height information of the Z-map contacting with the tool. For the voxel model, the interference area can be calculated by extracting the voxels existing in the tool, as shown in **Fig. 6(b)**. The change of the workpiece shape

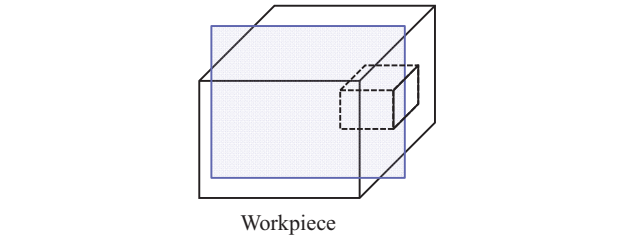

Fig. 5. Comparison of workpiece with overhangs between the contour line model and Z-map model.

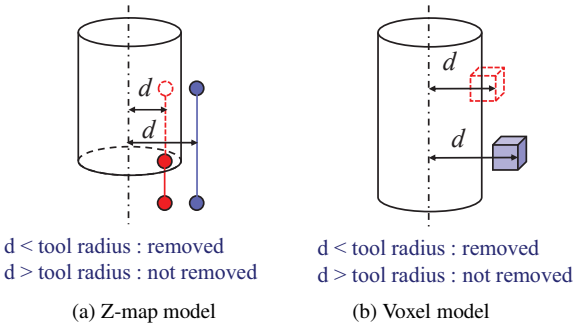

Fig. 6. Detection of interference area.

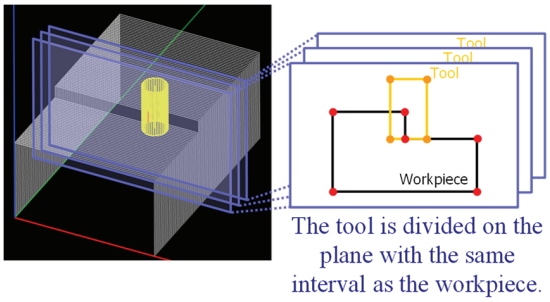

Fig. 7. Description of workpiece and tool with the contour line model.

can also be easily expressed by removing the voxels contacting with the tool.

In the contour line model, the interference area can be calculated using the following procedure. Firstly, the tool is divided on the plane with an interval similar to that of the workpiece, as shown in **Fig. 7**. For a square end mill, the tool is drawn as a rectangle on the plane. Next, the interference area is calculated by detecting the intersection points between the rectangular edge representing the tool and the polygon edge representing the workpiece,

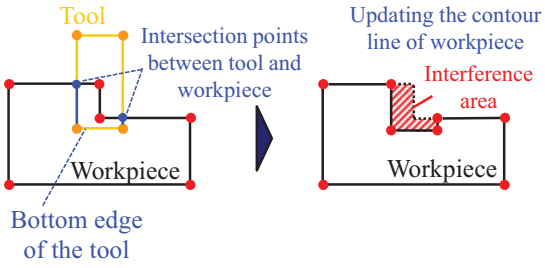

Fig. 8. Detection of intersection points and interference area between workpiece and tool.

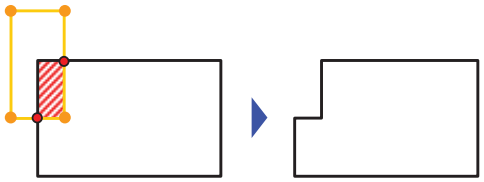

(a) Case when there is an intersection point at the bottom of the tool and an intersection point on the side of the tool

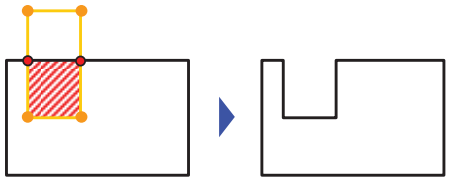

(b) Case when there are intersection points only on the side edge of the tool

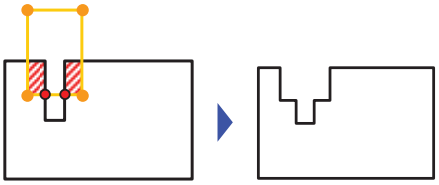

(c) Case when there are multiple intersection points at the bottom edge of the tool

Fig. 9. Pattern of positional relationship between workpiece and tool.

and extracting the area surrounded by the detected intersection points and the bottom edge of the rectangle representing the tool, as shown in **Fig. 8**. The pattern of the interference area between the rectangle and the polygon can be categorized into three different patterns, as shown in **Fig. 9**.

The first pattern is when there are intersection points at the bottom of the tool and on the side of the tool. In this case, the workpiece shape is changed by adding the intersection points and one bottom point of the tool as a point of the contour line of the workpiece and removing the points and edges existing inside the tool, as shown in **Fig. 9(a)**. The second pattern is when there are intersection points only on the side edge of the tool. In this case, the workpiece shape is changed by adding the intersection points and the bottom points of the tool as a point of the contour line of the workpiece and removing the points and

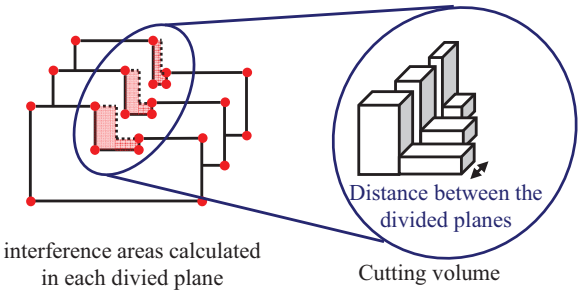

Fig. 10. Cutting volume calculated from interference area.

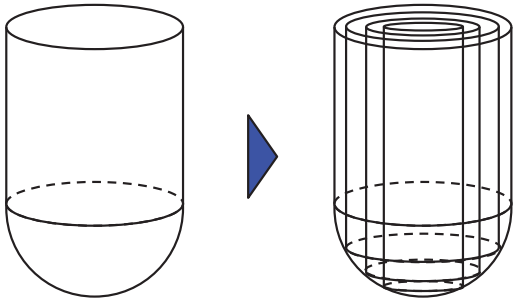

Fig. 11. Ball end mill expressed by superposition of square end mill.

edges existing inside the tool, as shown in **Fig. 9(b)**. The third pattern is when there are multiple intersection points at the bottom edge of the tool. In this case, the workpiece shape is changed by adding the intersection points and the bottom points of the tool as a point of the contour line of the workpiece and removing the points and edges existing inside the tool similar to the first pattern, as shown in **Fig. 9(c)**.

As described above, a 3-dimensional shape can be expressed by updating the contour line of the workpiece in each divided plane. Furthermore, the cutting volume during end milling can be calculated by multiplying the distance between the divided planes and the interference areas calculated in each divided plane and then, adding them together, as shown in **Fig. 10**.

2.3. Analysis for Various Tool Shapes

The proposed model analyzes by approximating a square end mill to a cylinder. It can also analyze tools, apart from that of the square end mill, by superpositioning the square end mill. For example, for a ball end mill, the tool can be discretely expressed by a plurality of square end mills where the tool diameter decreases in the direction of the tip, as shown in **Fig. 11**. The interference area between the tool and workpiece can be calculated by repeating in order from the largest tool diameter for a plurality of discretely expressed square end mills. Furthermore, various tool shapes, such as a bull nose end mill and tapered end mill, can also be applied by discretely representing with multiple square end mills, as shown in **Fig. 12**.

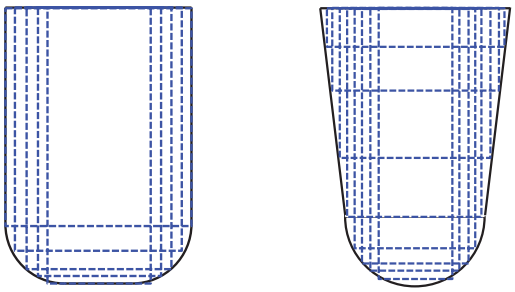

(a) Bull nose end mill (b) Tapered end mill

Fig. 12. Examples of expression with various tool shapes.

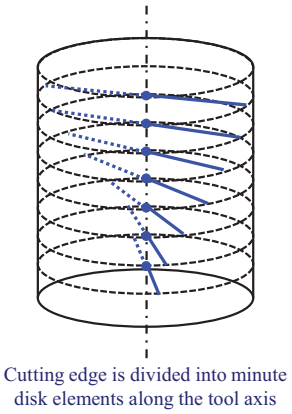

Fig. 13. Cutting edge in minute disk element of tool.

2.4. Prediction of Cutting Force

While the present study proposes a method to calculate the interference area between the tool and workpiece and update the workpiece shape during the end milling process, the instantaneous rigid force model [1–4] is applied for prediction of the cutting force. This model can accurately predict cutting forces in end milling based on the geometric relationship between the cutting edge and workpiece. Here, the cutting edge is divided into minute disk elements along the tool axis, as shown in **Fig. 13**. The minute cutting force acting on each disk element is calculated. Next, the total cutting force acting on the tool is calculated by adding the minute cutting force acting on each disk element. The minute cutting forces acting on each disk element, such as the tangential force dF_t, radial force dF_r, and axial force dF_a, are denoted by the following equations [23].

$$dF_t = \left[K_{te} + K_{tc}h(\theta,z)\right]dz, \quad \ldots\ldots\ldots \quad (1)$$

$$dF_r = \left[K_{re} + K_{rc}h(\theta,z)\right]dz, \quad \ldots\ldots\ldots \quad (2)$$

$$dF_a = \left[K_{ae} + K_{ac}h(\theta,z)\right]dz. \quad \ldots\ldots\ldots \quad (3)$$

In Eqs. (1)–(3), K_{te}, K_{re}, K_{ae}, K_{tc}, K_{rc}, and K_{ac} are the cutting parameters, $h(\theta,z)$ is the uncut chip thickness, and parameter dz is the thickness of the minute disk element. In the instantaneous rigid force model, cutting force is calculated using $h(\theta,z)$. In the present study, $h(\theta,z)$ of each minute disk element can be calculated from the distance at

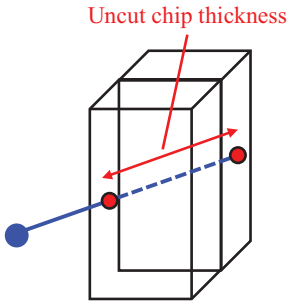

Fig. 14. Calculation of the uncut chip thickness.

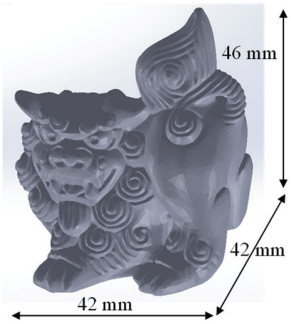

Fig. 15. 3D CAD model for case study.

which the cutting edge crosses the extracted interference area. As described in the Section 2.2, the interference area can be expressed using multiple cuboids. Therefore, $h(\theta, z)$ can be calculated from the intersection points between the cutting edge and the surface constituting the cuboid, as shown in **Fig. 14**.

3. Case Study

A case study was conducted to validate the effectiveness of the proposed model. An end milling simulation was performed for a 3-dimensional shape, and the predicted workpiece shape was compared with the machined shape and the memory usage during the simulation was verified. Furthermore, a cutting experiment using a square end mill was performed, and the cutting force measurements were compared with the predicted values.

3.1. End Milling Simulation for 3-Dimensional Shape

End milling simulation for a 3-dimensional shape, as shown in **Fig. 15**, was conducted to validate the effectiveness of the proposed model. The 3-dimensional model was in the STL format obtained by photographing the product shape, as shown in **Fig. 16**, with a 3-dimensional scanner (Shining 3D, EinScan-SE). In the end milling simulation, rough cutting was performed using a square end mill with a tool diameter of 6 mm, and finish cutting was performed using a ball end mill with a tool diameter of 6 mm. The simulation conditions are listed in **Table 1**.

Fig. 16. Original product for case study.

Table 1. End milling simulation condition for case study.

Rough cutting	Axial depth of cut	2.0 mm
	Radial depth of cut	1.0 mm
	Spindle speed	3000 min^{-1}
	Feed rate	600 mm/min
Finish cutting	Axial depth of cut	2.0 mm
	Radial depth of cut	0.5 mm
	Spindle speed	3000 min^{-1}
	Feed rate	600 mm/min

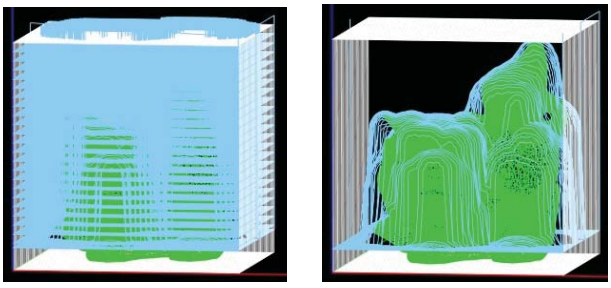

(a) Rough cutting (b) Finish cutting

Fig. 17. Tool paths generated for case study.

During simulation, the tool path used was calculated using the computer-aided manufacturing (CAM) software (BESTOWS Milling, BESTOWS Co., Ltd). **Fig. 17** shows the tool paths used for this case study. To qualitatively evaluate the 3-dimensional shape predicted by the proposed model, the workpiece was machined using aluminum A5052 as the material with a vertical type machining center (NMV1500DCG, DMG Mori Co., Ltd.). **Fig. 18** shows the workpiece after machining. **Fig. 19** shows the results of the proposed contour line model. The proposed model was validated based on the results that show that the predicted shape was almost similar to the actual machined shape. Furthermore, the memory usage after rough cutting (**Fig. 19(a)**) was 285 MB when the simulation was conducted with an analysis resolution of 500 μm. Thus, the proposed model is recommended for practical applications.

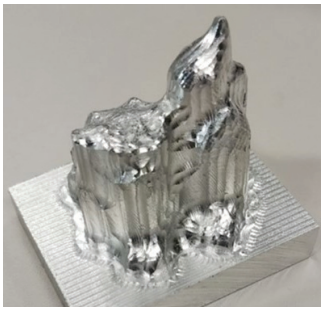

Fig. 18. Workpiece after machining.

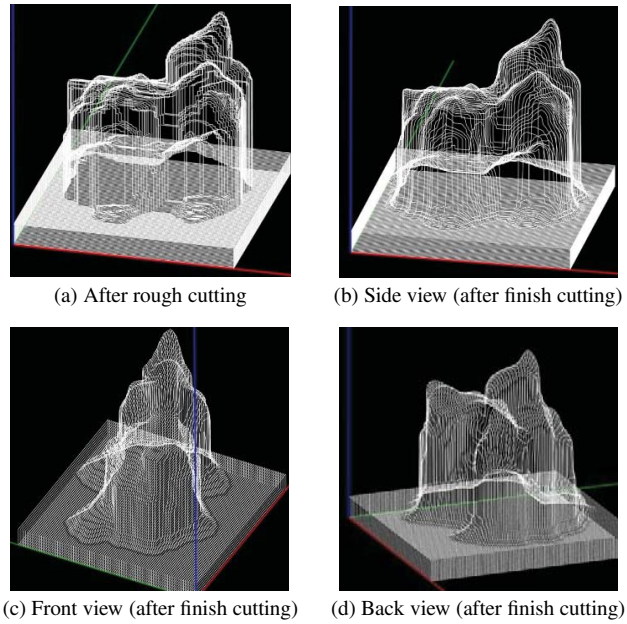

(a) After rough cutting (b) Side view (after finish cutting)

(c) Front view (after finish cutting) (d) Back view (after finish cutting)

Fig. 19. Simulation result of workpiece shape.

3.2. Cutting Force Simulation

A cutting experiment was conducted with the square end mill. The experimentally measured cutting force was compared with the cutting force predicted by the proposed model. The cutting conditions and cutting force simulation conditions are listed in **Table 2**. The machining was conducted by a vertical type machining center (NMV1500DCG) and the cutting force was measured with a dynamometer (KISTLER 9257B). For the cutting force simulation, the cutting parameters for the instantaneous rigid force model were determined through a preliminary experiment [23]. The determined cutting parameters are listed in **Table 3**.

The result of the measured cutting force and the predicted cutting force is shown in **Fig. 20**. Based on the result, it can be confirmed that the variation of the measured and predicted results agree well, although there is a difference in the cutting force peak or the variation near the start and the end of cutting. A reason for this difference could be the interval of the divided planes that indicates resolution. In the case study, interval of the divided ZX-planes was 25 μm. Therefore, it can be considered

Table 2. Cutting condition and cutting force simulation condition.

Machine tool		NMV1500DCG
Workpiece		A5052
Cutting tool	Tool type	Square end mill
	Helix angle	30°
	Number of flutes	2
	Diameter	6.0 mm
Cutting conditions	Cutting direction	Up cut
	Axial depth of cut	3.0 mm
	Radial depth of cut	3.0 mm
	Spindle speed	2000 min^{-1}
	Feed rate	200 mm/min
Disk element thickness of tool		0.025 mm
Interval of contour line		0.025 mm

Table 3. Determined cutting coefficients.

Cutting coefficients	K_{te}	0.5 N/mm
	K_{tc}	1323.7 N/mm
	K_{re}	0.4 N/mm
	K_{rc}	792.2 $\mathrm{N/mm}^2$
	K_{ae}	3.1 $\mathrm{N/mm}^2$
	K_{ac}	81.6 $\mathrm{N/mm}^2$

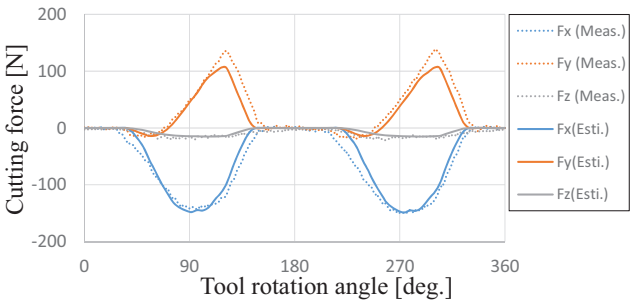

Fig. 20. Measured and predicted cutting force using square end mill.

that the calculated uncut chip thickness was slightly different than the actual one and thus, an error occurred in the cutting force peak. Another reason could be the disregard of tool deflection. A previous study [20] showed that the tool deflects toward the overcut direction when the cutting direction is up cut. Hence, it is understood that the calculated uncut chip thickness was slightly different from the actual one and thus, an error occurred in the cutting force peak. Furthermore, the reason for this is considered to be the analysis time resolution. In this case study, the uncut chip thickness was calculated for each feed per tooth while considering the tool shape as a cylinder. In actual practice, the cutting edge moves as a trochoid instead of arcs. Therefore, it is considered that an error occurred in the cutting force near the start and end of cutting. However, it was confirmed that cutting force prediction using

the proposed model was performed as well as its practical usage.

4. Conclusions

In the present study, a contour line model for end milling simulation was proposed to realize high-speed arithmetic processing by reducing memory usage. The contour line model was realized as follows:

1. A 3-dimensional shape was expressed by superimposing the contour line of the cross-sections obtained by dividing the workpiece along any axial direction.
2. Cutting volume was obtained by calculating the interference area between the contour line of the workpiece on the divided plane and the rectangle extracted from the cross-section of the tool. Furthermore, the workpiece shape could be changed according to the interference area.
3. Cutting force was predicted using the uncut chip thickness for each cutting edge from the positional relationship between the interference area and the cutting edge.

In the case study, the cutting experiment and comparison between the machined shape and the prediction result confirmed that the prediction result from the proposed model was accurate. Furthermore, a comparison between the measured and predicted cutting forces, confirmed that the cutting force prediction in the proposed model was performed correctly.

Acknowledgements

This work has been partially supported by the Machine Tool Engineering Foundation and Osawa Scientific Studies Grants Foundation. Further, the authors of the paper would like to acknowledge the support from the Machine Tool Technologies Research Foundation (MTTRF).

References:

[1] J. Tlusty and P. MacNeil, "Dynamics of Cutting Forces in End Milling," CIRP Annals, Vol.24, No.1, p. 21, 1975.
[2] D. Mongomery and Y. Altintas, "Mechanism of cutting force and surface generation in dynamic milling," J. of Engineering for Industry, Vol.113, No.2, p. 21, 1991.
[3] Y. Altintas and P. Lee, "A General Mechanics and Dynamics Model for Helical End Mills," CIRP Annals, Vol.45, No.1, p. 59, 1996.
[4] K. Shirase and Y. Altintas, "Cutting force and dimensional surface error generation in peripheral milling with variable pitch helical end mills," Int. J. of Machine Tools and Manufacture, Vol.36, No.5, pp. 567-584, 1996.
[5] T. Matsumura, T. Furuki, and E. Usui, "Prediction of Cutting Process with Curved-Edge End Mill (1st Report)," The Japan Society of Mechanical Engineers, Vol.69, No.688, pp. 3396-3402, 2003.
[6] W. Ferry and D. Yip-Hoi, "Cutter-workpiece engagement calculations by parallel slicing for five-axis flank milling of jet engine impellers," ASME J. of Manufacturing Science and Engineering, Vol.130, No.5, 051011, 2008.
[7] A. D. Spence and Z. Li, "Parallel Processing for 2-1/2D Machining Simulation," Proc. of the 6th ACM Symp. on Solid Modeling and Applications (SMA '01), pp. 140-148, 2001.
[8] T. Nishikawa, K. Kikuta, M. Mondou, T. Tsutsumoto, and J. Kaneko, "Machining Error Compensation System in End Milling," J. of the Japan Society for Precision Engineering, Vol.78, No.11, pp. 975-979, 2012.
[9] Y. Takeuchi, M. Sakamoto, Y. Abe, R. Orita, and T. Sata, "Development of a personal CAD/CAM system for mold manufacture based on solid modeling techniques," CIRP Annals, Vol.38, No.1, p. 429, 1989.
[10] M. Inui, "Fast Simulation of Sculptured Surface Milling with 3-Axis NC Machine," Trans. of Information Processing Society of Japan, Vol.40, No.4, pp. 1808-1815, 1999.
[11] A. Sullivan, H. Erdim, R. Perry, and S. Frisken, "High Accuracy NC Milling Simulation Using Composite Adaptively Sampled Distance Fields," J. of Computer-Aided Design, Vol.44, pp. 522-536, 2012.
[12] T. Kishinami, S. Kanai, H. Shinjo, H. Nakahara, and K. Saito, "An application of voxel representation to machining simulator," J. of the Japan Society for Precision Engineering, Vol.55, No.1, pp. 105-110, 1989.
[13] M. Balasuabramaniam, P. Laxmiprasad, S. Sarma, and Z. Shaikh, "Generating 5-axis NC roughing paths directly from a tessellated representation," Computer-Aided Design, Vol.32, No.4, pp. 261-277, 2000.
[14] S. Hauth, Y. Murtezaoglu, and L. Linsen, "Extended linked voxel structure for point-to-mesh distance computation and its application to NC collision detection," Computer-Aided Design, Vol.41, No.12, pp. 896-906, 2009.
[15] T. Hasegawa, R. Sato, and K. Shirase, "Cutting Force Simulation Referring Workpiece Voxel Model for End-milling Operation and Adaptive Control Based on Predicted Cutting Force," J. of the Japan Society for Precision Engineering, Vol.82, No.5, pp. 467-472, 2016.
[16] M. Inui and N. Umezu, "Implementation of a 5-Axis Milling Simulation System Using Triple Dexel Models," J. of the Japan Society for Precision Engineering, Vol.76, No.3, pp. 361-366, 2010.
[17] Y. Tsuchitana, J. Kaneko, and K. Horio, "Fast Simulation Algorithm of Voxel Representation Method for Multi Axis Control Machining," J. of the Japan Society for Precision Engineering, Vol.79, No.5, pp. 467-472, 2013.
[18] I. Nishida, R. Sato, and K. Shirase, "High Speed Computational Algorithm in Voxel Based Milling Process Simulation for Minute Time and Minute Space Resolution Analysis," J. of the Japan Society for Precision Engineering, Vol.84, No.2, pp. 175-181, 2018.
[19] I. Nishida, R. Okumura, R. Sato, and K. Shirase, "Cutting Force Simulation in Minute Time Resolution for Ball End Milling Under Various Tool Posture," J. of Manufacturing Science and Engineering (ASME), Vol.140, No.2, 021009, 2017.
[20] I. Nishida, R. Okumura, R. Sato, and K. Shirase, "Voxel Based End-milling Simulation Considering Elastic Deflection of Tool System," J. of the Japan Society for Precision Engineering, Vol.84, No.6, pp. 572-577, 2018.
[21] I. Nishida and K. Shirase, "Machining Error Correction Based on Predicted Machining Error Caused by Elastic Deflection of Tool System," J. of the Japan Society for Precision Engineering, Vol.85, No.1, pp. 91-97, 2019.
[22] I. Nishida, R. Tsuyama, R. Sato, and K. Shirase, "Customized End Milling Operation of Dental Artificial Crown without CAM Operation," Int. J. Automation Technol., Vol.12, No.6, pp. 947-954, 2018.
[23] H. Narita, "A Determination Method of Cutting Coefficients in Ball End Milling Forces Model," Int. J. Automation Technol., Vol.7, No.1, pp. 39-43, 2013.

Name:
Isamu Nishida

Affiliation:
Assistant Professor, Department of Mechanical Engineering, Graduate School of Engineering, Kobe University

Address:
1-1 Rokko-dai, Nada, Kobe 657-8501, Japan

Brief Biographical History:
2012- Sysmex Corp.
2016- Assistant Professor, Kobe University
2018- CEO, BESTOWS Co., Ltd. (Concurrently)

Main Works:
• "Machine tool assignment realized by automated NC program generation and machining time prediction," Int. J. Automation Technol., Vol.13, No.5, pp. 700-707, 2019.
• "Sequence planning of on-machine measurement and re-machining," J. of Advanced Mechanical Design, Systems, and Manufacturing, Vol.13, No.1, JAMDSM0014, 2019.
• "Customized End Milling Operation of Dental Artificial Crown without CAM Operation," Int. J. Automation Technol., Vol.12, No.6, pp. 947-954, 2018.

Membership in Academic Societies:
• Japan Society of Mechanical Engineers (JSME)
• Japan Society for Precision Engineering (JSPE)

Name:
Keiichi Shirase

Affiliation:
Professor, Department of Mechanical Engineering, Graduate School of Engineering, Kobe University

Address:
1-1 Rokko-dai, Nada, Kobe 657-8501, Japan

Brief Biographical History:
1984- Research Associate, Kanazawa University
1995- Associate Professor, Kanazawa University
1996- Associate Professor, Osaka University
2003- Professor, Kobe University

Main Works:
• K. Shirase and K. Nakamoto, "Simulation Technologies for the Development of an Autonomous and Intelligent Machine Tool," Int. J. Automation Technol., Vol.7, No.1, pp. 6-15, 2013.
• T. Kobayashi, T. Hirooka, A. Hakotani, R. Sato, and K. Shirase, "Tool Motion Control Referring to Voxel Information of Removal Volume Voxel Model to Achieve Autonomous Milling Operation," Int. J. Automation Technol., Vol.8, No.6, pp. 792-800, 2014.
• M. M. Isnaini, Y. Shinoki, R. Sato, and K. Shirase, "Development of CAD-CAM Interaction System to Generate Flexible Machining Process Plan," Int. J. Automation Technol., Vol.9, No.2, pp. 104-114, 2015.
• K. Shirase, "CAM-CNC integration for innovative intelligent machine tool," Proc. of the 8th Int. Conf. on Leading Edge Manufacturing in 21st Century (LEM21), A01, 2015.
• I. Nishida, R. Okumura, R. Sato, and K. Shirase, "Cutting Force Simulation in Minute Time Resolution for Ball End Milling Under Various Tool Posture," ASME J. of Manufacturing Science and Engineering, Vol.140, No.2, 021009, 2018.

Membership in Academic Societies:
• American Society of Mechanical Engineers (ASME)
• Society of Manufacturing Engineers (SME)
• Japan Society of Mechanical Engineers (JSME), Fellow
• Japan Society for Precision Engineering (JSPE), Fellow